JOURNAL OF APPLIED POLYMER SCIENCE VOL. 15, PP. 2791–2805 (1971)

The Rheology of Filled Polymers

N. J. MILLS,* *Imperial Chemical Industries Limited, Petrochemical & Polymer Laboratory, The Heath, Runcorn, Cheshire, England*

Synopsis

The flow properties of polymer melts containing fillers of various shapes and sizes have been examined. If there is no failure of either the filler or polymer in the solid state, then the modulus enhancement for randomly distributed filler is equal to the melt viscosity enhancement under medium shear stress conditions (10^4 Nm^{-2}) in simple shear flow or in oscillatory shear flow. Submicron-size fillers, in particular, can form weak structures in the melt that greatly increase the low shear rate viscosity without changing the modulus of the solid proportionately. The highly pseudo-plastic nature of polymer melts at shear stresses of 10^6 Nm^{-2} means that, even without orientation of filler particles toward the flow direction, the viscosity enhancement is less than at lower shear stresses.

INTRODUCTION

The use of inorganic fillers of various kinds in polymers has become common, and the mechanical properties of the composites are fairly well understood. Far less is known of how a filler modifies the flow properties of a polymer. Usually when the use of fillers is considered, a compromise has to be made between improved mechanical properties in the solid state, the increased difficulty of melt processing, the problem of dispersing filler in the polymer, and the economics of the process. Therefore it is important to know the relationship between filler concentration and geometry and the flow properties of the composite.

There is a theoretical correspondence between slow viscous flow of a liquid and the infinitesimal strain elasticity of a solid. This has been used[1] to predict that the viscosity η of liquid containing filler and the shear modulus G of a solid containing an identical distribution of rigid filler are related to the quantities for the unfilled matrix η_0, G_0 by

$$\eta/\eta_0 = G/G_0. \tag{1}$$

In the case of thermoplastics, the same system can easily be studied in both the solid and liquid states, and conditions for the validity of this equality are established in this paper. Useful predictions about solid composites may then be made from the study of filled liquids and vice versa.

It is known qualitatively from the study of postextrusion swelling[2] of filled polymers that the melt elasticity decreases with increasing filler con-

* Present address: Dept. of Physical Metallurgy and Science of Materials, University of Birmingham, Birmingham, B15 2TT, England.

tent. An attempt was made to measure melt elasticity quantitatively and correlate the effects of such changes.

THEORY

Thomas[3] has reviewed the investigations of the viscosity of suspensions of spheres in Newtonian (constant viscosity) media. After allowing for effects of sphere size, he showed that the viscosity increase in a medium containing a volume fraction ϕ of uniform-sized spheres is

$$\frac{\eta}{\eta_0} = 1 + 2.5\phi + 10.05\phi^2 + 0.00273 \exp(16.6\phi) \qquad \text{for } 0 < \phi < 0.6 \quad (2)$$

The second term on the right-hand side of eq. (2) is due to Einstein,[4] the third to Manley and Mason,[5] and the fourth is empirical. If the condition of uniform-sized spheres is relaxed, eq. (2) overestimates the suspension viscosity. Farris[6] predicts that for a bimodal-size distribution of spheres with a diameter ratio greater than 10, there is zero interaction between the two sizes, and the viscosity of the suspension is the product of two terms given separately by eq. (2) for the partial volume fractions.

There are exact theories[7] for the viscosity of very dilute suspensions of ellipsoids and rods, but none for the higher concentration region. The semiempirical theories of Robinson[8] and Mooney[9] for concentrated suspensions of spheres may be of some help in the analysis of data for nonspherical fillers. Thus, Brodnyan[10] has used the equation

$$\frac{\eta}{\eta_0} = \exp\left(\frac{2.5\phi + 0.399\phi(p-1)^{1.48}}{1 - K\phi}\right) \quad (3)$$

to describe the viscosity of suspensions of rods with axial ratio p for $\phi <$ 0.01. The constant K tends toward 1.91 as p increases.

If eq. (1) is valid, then theories such as Kerner's for the shear modulus of a suspension of grains that are in the mean spherical can be applied to the viscosity of filled polymers. If the polymer has shear modulus G_0 and Poisson's ratio ν and contains a volume fraction ϕ of filler with shear modulus G_2, then the composite shear modulus G is given by

$$\frac{G}{G_0} = \frac{\dfrac{G_2\phi}{(7-5\nu)G_0 + (8-10\nu)G_2} + \dfrac{1-\phi}{15(1-\nu)}}{\dfrac{G_0\phi}{(7-5\nu)G_0 + (8-10\nu)G_2} + \dfrac{1-\phi}{15(1-\nu)}}. \quad (4)$$

This result is identical to the lower bound of the elastic modulus of quasi-isotropic and quasi-homogeneous two-phase materials of arbitrary geometry calculated by Hashin and Shtrikman.[12] For a polymer melt, $\nu = 0.5$, and the modulus ratio G_2/G_0 is effectively infinite for most fillers. Applying eq. (1), we have from eq. (4), therefore,

$$\frac{\eta}{\eta_0} = 1 + \frac{2.5\phi}{1-\phi}. \quad (5)$$

Polymer melts generally have apparent viscosities that decrease with increasing rate of shear in steady shear flow and show a number of elastic properties reminiscent of those of rubbers. Under high shear stresses, the melt becomes anisotropic in its properties. This corresponds to an alignment of polymer molecules from random coil configurations at rest into ellipsoidal shapes partially oriented toward the flow direction. It is only at low shear rates in simple shear flow, or at low frequencies in oscillatory shear flow when the polymer response is mainly a viscous one (the Newtonian flow region is being approached), that eqs. (2) or (5) are expected to be valid.

One particular molecular theory has been used to interpret the low stress behavior of polymer melts. In this, the elastic liquid theory of Lodge,[13] the melt is treated as if it contained transient rubber networks that are continually breaking and reforming. These "entanglement" networks are characterized by an entanglement lifetime function $\mu(\tau)$, where τ is the time for which an entanglement has existed. Rheological quantities such as the shear modulus G_I for an instantaneous small strain and the in-phase and out-of-phase components G' and G'' of the complex shear modulus G^* for a sinusoidal strain are given by

$$G_I = \int_0^\infty \mu(\tau)d\tau \tag{6}$$

$$\lim_{\omega \to 0} \frac{G''}{\omega} = \int_0^\infty \mu(\tau)\tau d\tau = \eta_0 \tag{7}$$

$$\lim_{\omega \to 0} \frac{G'}{\omega^2} = \int_0^\infty \mu(\tau)\tau^2 d\tau = \eta_0^2 J \tag{8}$$

where ω is the angular frequency, η_0 is the viscosity in steady shear flow, and J is the "steady state shear compliance." Fillers could change the entanglement lifetime function either through hydrodynamic effects or by chemical interaction with the polymer.

Although eq. (7) only applies to polymers when they behave as Newtonian liquids, it has been observed[14] that the steady shear apparent viscosity η_a at shear rate $\dot{\gamma}$ is equal to the magnitude of the oscillatory viscosity:

$$\eta_{a_{\dot{\gamma}=\omega}} = |\eta^*| = \frac{|G^*|}{\omega}. \tag{9}$$

EXPERIMENTAL

Techniques

Melt viscosities in steady flow shear were measured with both a Weissenberg rheogoniometer cone-and-plate viscometer (Model R16 manufactured by Sangamo Controls Ltd., cone diameter 2.5 cm and 4° angle, cone truncated by 178 μm) and, at higher shear rates, with a small capillary viscometer.[15] Two capillary lengths of the same diameter were used so that cor-

rections could be made for pressure losses near the capillary entrance. The melts were also studied in the Weissenberg rheogoniometer with the same cone-and-plate platens, using a sinusoidal strain input of amplitude 0.12. The piezoelectric measuring head and transfer function analyzer used in oscillatory shear measurements have been described previously.[16] Steady shear measurements could only be made in the cone-and-plate viscometer for the polymers studied for shear rates less than 0.5 sec^{-1}. Above this value, material is ejected from the gap and decreasing torque readings are obtained. This difficulty did not occur with oscillatory shear measurements. No degradation of the polymers occurred, identical results being obtained at the beginning and end of testing.

Stress–strain measurements were made on some of the composites using a Hounsfield E tensile testing machine, with a 1-in. gauge length extensometer for strain measurement, at a strain rate of 5%/min. Shear moduli of some solid composites were also measured using an air-bearing torsion pendulum at a frequency ~3 sec^{-1} and maximum shear strain of 10^{-4}. Note that throughout this paper frequency means angular frequency in radians/sec.

Composites

Table I lists the combinations of polymer and filler used and the method of preparation of the composites.

TABLE I
Composite Formulation

Filler				
Shape	Material	Size	Polymer[e]	Mixing method
Sphere	glass[a]	130 μm	polystyrene Carinex MW	dry blend—injection mold
Rod	"E" glass[b]	6 mm × 15 μm	H.D. polyethylene Rigidex 2	Frenkel mixer[f]
Rod	nylon 6	1.5 mm × 50 μm	polystyrene Carinex MW	dry blend—compression mold
	nylon 6	600 μm × 20 μm	polystyrene anionic	solution blend—compression mold
Platelets aspect ratio ~5:1	kaolin[c]	50% < 0.7 μm range 0.1–10 μm	L.D. polyethylene Alkathene XDG58	twin-roll mill
Irregular	colloidal silica[d]	4 nm	L.D. polyethylene Alkathene XRM21	Brabender internal mixer

[a] Ballotini Manufacturing Co. Ltd., Barnsley, Yorks.
[b] Length after mixing given in Table II.
[c] English China Clays, Speswhite (SDS).
[d] British Drug House.
[e] The Carinex polystyrene was in the form of beads of roughly 400 μm diameter, and the polyethylenes were in granular form.
[f] The Frenkel mixer is a small extruder, the output of which passes through a 1-mm diameter die.

RESULTS

Spherical Filler

Figure 1 shows the complex shear modulus data versus frequency for the polystyrene with different loadings of glass spheres. A comparison of the dynamic shear modulus of injection-molded unfilled polystyrene with a sample compression-molded under a vacuum showed that there had been negligible degradation of the polystyrene during fabrication. The effect of increasing the ϕ of glass spheres is to increase G' and G'' in equal ratios at a given frequency, so that the frequency at which G' equals G'' stays constant. The unfilled polystyrene shows the beginning of the rubbery plateau region for G'' at a level of 5×10^4 Nm^{-2}. This level is characteristic of the entanglement network of polystyrene[17] and extends to the frequency ($\sim 10^4$ sec^{-1} at 190°C) where the glass transition begins. The rise in the plateau level with addition of filler can be interpreted as the entanglement network being reinforced by the glass spheres. For unfilled polymers, the effect of a change of temperature, or of molecular weight if the molecular weight distribution width is the same, is to shift the log complex shear modulus versus log frequency curves along the frequency axis. The addition of a volume fraction ϕ of filler apparently increases each of the three quantities in eqs. (6) to (8) by a factor $K(\phi)$. Hence the melt compliance measured either as $1/G'$ (plateau) (see Ferry[18]) or as the steady shear compliance $J = \text{Lim}_{\omega \to \infty} (G'/G''^2)$ decreases as $1/K(\phi)$.

Steady shear measurements made by Newman and Trementozzi[2] on polystyrene–acrylonitrile containing glass beads show approximately equal viscosity increases at a shear rate of 3 sec^{-1} (Fig. 2) to our oscillatory data.

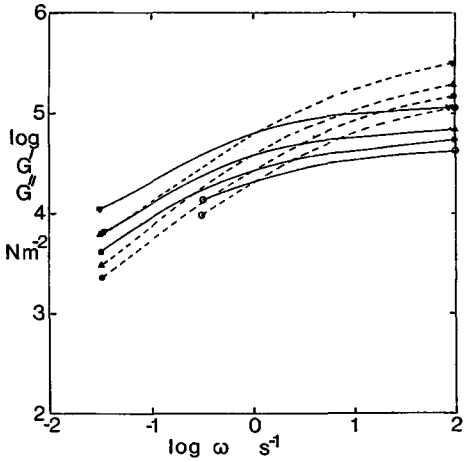

Fig. 1. Log G'' (solid lines) and G' (dashed lines) vs. log frequency for polystyrene containing glass sphere at 190°C: (O) $\Phi = 0$; (●) $\Phi = 0.092$; (▲) $\Phi = 0.223$; (▼) $\Phi = 0.411$. For clarity, in this figure and in figs. 3, 6, and 10, experimental points have been omitted. Data were taken at intervals of 0.3 in log ω (0.5 in Figs. 3, 6, 10), and the curved lines through these points are shown.

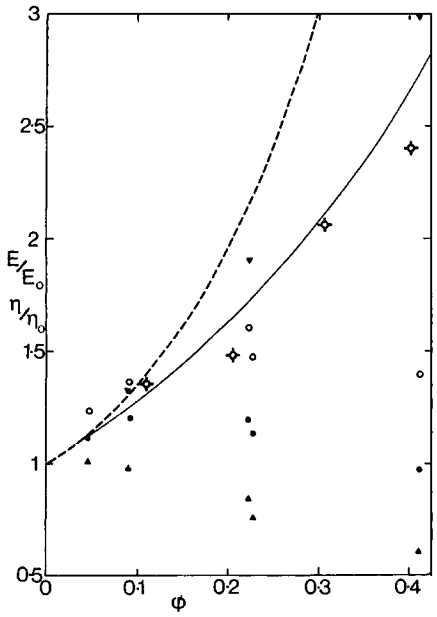

Fig. 2. Viscosity and modulus ratios vs. Φ of glass spheres in polystyrene E/E_0 at 20°C: (○) 0.001 strain; (●) 0.003 strain; (▲) 0.010 strain; (▼) $|\eta^*|/|\eta^*_0|$ at 190°C and $1s^{-1}$; (⊖) η_a/η_{a0} at 204°C and 3 sec^{-1} (ref. 2). Solid line, eq. (5), dashed line, eq. (2).

This increase is less at higher shear rates and may be higher in the Newtonian flow region. The viscosity data in Figure 2 falls between the lines for eqs. (2) and (5). Apart from when the volume fraction of glass was low, the Young's modulus ratios for the composites fall well below the viscosity ratios in Figure 2. The Young's modulus decreased with increasing strain up to 1%, but on unloading from this strain the modulus remained approximately constant. The initial reinforcement did not occur on reloading. It is suggested that some factor, possibly the molded-in orientation of the polystyrene or the differential contraction of glass and polystyrene on cooling from T_g, causes failure to occur at or near the polystyrene–glass interface at low strains. This effect occurs at lower strain levels the higher the volume fraction of spheres. After this failure, the composite is similar to a polystyrene foam with $E/E_0 \simeq 1 - \phi$. When glass spheres having different surface treatments to vary adhesion were embedded in epoxy resin[19] (no matrix orientation or thermal contraction stresses), the composite modulus followed Kerner's theory. The same was true of low-strain shear moduli measurements of glass spheres in phenoxy thermoplastic.[20] Therefore this failure is not a general phenomenon.

Rod-Shaped Fillers

When glass fiber of $^1/_4$-in. length was mixed with high-density polyethylene in an extruder, considerable breakage of the fiber occurred. Some of

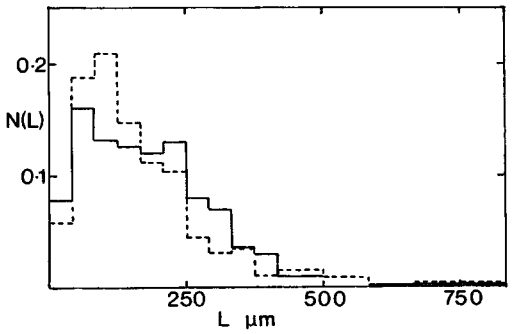

Fig. 3. Number fraction of glass fibers in polyethylene within length categories. Solid lines, $\Phi = 0.04$; dashed lines, $\Phi = 0.19$.

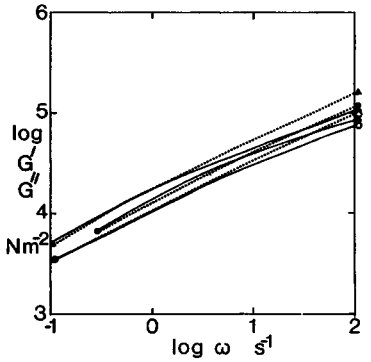

Fig. 4. Log G'' (solid lines) and G' (dashed lines) vs. log frequency for glass fibers in polyethylene at 190°C: (○) $\Phi = 0$; (●) $\Phi = 0.10$; (▲) $\Phi = 0.19$.

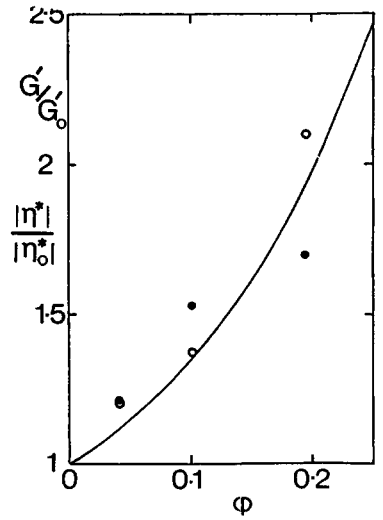

Fig. 5. Viscosity and modulus ratios vs. Φ of glass fiber in polyethylene: (○) G'/G_0' at 30°C, 3 sec^{-1}; (●) $|\eta^*|/|\eta_0^*|$ at 190°C, 1 sec^{-1}. Solid line, eq. (2).

the granulated composite was extracted in a Soxhlet extractor with xylene, and the glass fiber was examined under an optical microscope. Figure 3 shows the fiber length distribution. This type of length distribution is typical in glass fiber-filled thermoplastics.[21]

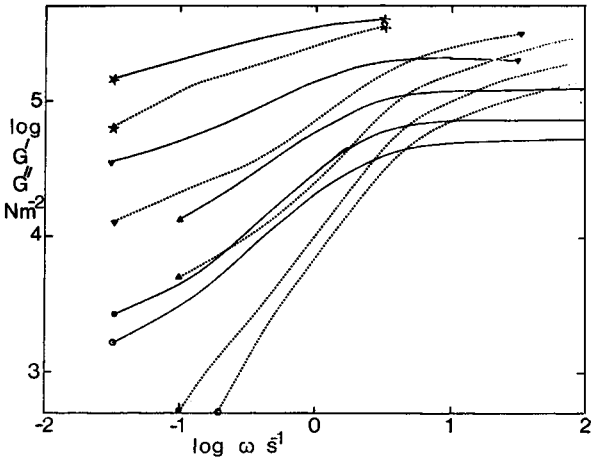

Fig. 6. Log G'' (solid lines) and G' (dashed lines) vs. log frequency for nylon fibers in anionic polystyrene at 901°C: (○) $\Phi = 0$; (●) $\Phi = 0.10$; (▲) $\Phi = 0.20$; (▼) $\Phi = 0.30$; (★) $\Phi = 0.40$.

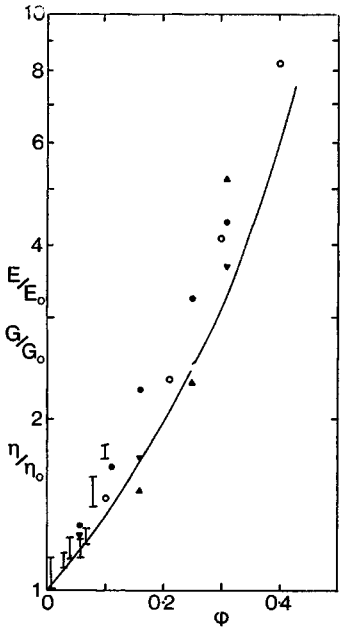

Fig. 7. Viscosity and Young's modulus ratios vs. filler content: (○) anionic polystyrene/nylon fibers G'' plat/G'' plat$_0$ at 190°C; (●) polyethylene/kaolin E/E_0 at 0.01 strain 20°C; (▼) η_a/η_{a0} 1 sec^{-1} at 190°C; (▲) $|\eta^*|/|\eta_0^*|$ 1 sec^{-1} at 190°C; (I) polyethylene/silica E/E_0 at 0.01 strain 20°C.

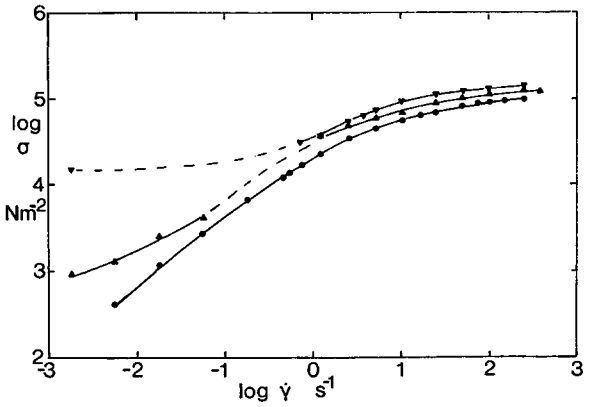

Fig. 8. Log shear stress vs. log shear rate for nylon fibers in Carinex polystyrene at 190°C: (○) $\Phi = 0$; (▲) $\Phi = 0.19$; (▼) $\Phi = 0.38$.

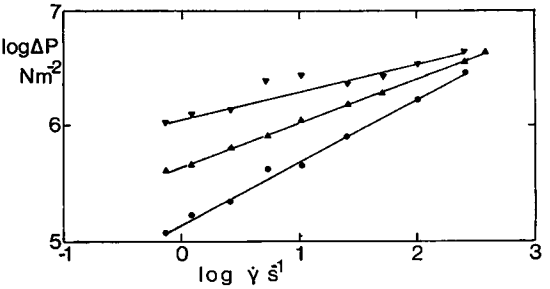

Fig. 9. Capillary viscometer and pressure correction vs. shear rate for nylon fibers in Carinex polystyrene at 190°C. Symbols as in Fig. 7.

Samples of the glass fiber–polyethylene composites were compression molded under vacuum, and then oscillatory shear measurements were made at 190°C. Figure 4 shows the complex shear modulus-versus-frequency results. The results for $\phi = 0.05$ have been omitted as they fall midway between $\phi = 0$ and $\phi = 0.10$ and are very similar. The broad molecular weight distribution of the polyethylene (gel permeation chromatography results give $\bar{M}_n = 7.4 \times 10^3$, $\bar{M}_w = 2.3 \times 10^5$, $\bar{M}_z = 2.3 \times 10^6$) means that G' and G'' stay comparable in magnitude throughout the frequency range. As in the polystyrene–glass spheres case, at a given frequency both G' and G'' are increased in the same ratio.

Continuous shear measurements with a capillary viscometer (not shown) give an apparent viscosity enhancement factor at $\phi = 0.20$ of 1.5 at shear rate 30 sec^{-1} and 1.4 at 900 sec^{-1} (the shear stress for the polymer alone was 100 and 300 kNm^{-2}, respectively, at the two shear rates).

Compression-molded bars of the glass-filled polyethylene were annealed at 100°C, and then the shear modulus was measured at 30°C with a torsion pendulum. The shear modulus enhancement factors in the solid state and the viscosity data are shown in Figure 5 to be given approximately by

eq. (2). Tensile modulus experiments at room temperature and 0.005 strain gave the same modulus enhancement factors, although the Young's moduli measured were nearly the same as the shear moduli at $\sim 10^{-4}$ strain, showing the nonlinear elasticity of polyethylene.

To overcome the variation in fiber length distribution in glass fiber-filled polyethylene, composites of polystyrene and nylon fibers cut to a uniform length were made. At 190°C, the shear modulus of the nylon is 2×10^8 Nm^{-2} measured with a torsion pendulum at low strains. The fibers are not broken during compression molding, and they were tested either under oscillatory shear in the Weissenberg rheogoniometer (random orientation of fibers) or in continuous shear (increasing orientation with increasing shear rate, particularly in the capillary flow case where the extensional flow above the capillary entrance aligns the fibers along the flow direction).

Oscillatory shear results on the anionic polystyrene–nylon fibers are shown in Figure 6. For $\phi = 0.10$, there is only a vertical shift of the curves, with no change of shape. However, at higher filler contents, the slopes of both $\log G'$ and $\log G''$ versus $\log \omega$ decrease for $\omega < 1$ sec^{-1}. At frequencies above 10 sec^{-1} G'' shows the typical plateau behavior of a high molecular weight narrow-distribution polystyrene. The increase in this plateau level with increasing ϕ is shown in Figure 7 to be slightly higher than the viscosity increase for the same volume fraction of monodisperse spheres, eq. (2). It is not realistic to characterize the changes in G'' and G' at low frequencies as changes in the viscosity of the composite since such behavior is not that of a Newtonian liquid. Rather, it implies that a weak three-dimensional network is formed between touching nylon fibers, this network only having relaxation mechanisms at long times.

Continuous shear measurements at 190°C with the Carinex polystyrene and larger nylon fibers (same length/diameter ratio) are shown in Figure 8. Again, the Newtonian region disappears for $\phi > 0.20$. At $\phi = 0.40$, there appears to be a definite yield stress of 1.5×10^4 Nm^{-2} for flow to occur. However, the increases in shear stress in steady flow at low shear rates are not as great as the corresponding changes in complex shear modulus. The capillary flow experiments at shear rates of 1 sec^{-1} and above show that the shear stress increase because the fiber is small, being only 1.4 at ~ 300 sec^{-1} and $\phi = 0.40$. The computed pressure drop just above the capillary entrance is shown as a function of shear rate in Figure 9. The extra pressure drop due to the presence of fibers does not increase as rapidly as that for the polymer alone with increased shear rate. A certain pressure drop is required to orient the fibers from their initially random configuration, and the effect of the oriented fibers on the flow properties just above and in the capillary is not very large.

Platelet-Shaped Particles

The kaolinite consists of hexagonal plate-like particles of low aspect ratio ($\sim 5:1$). Oscillatory shear results (Fig. 10) on carefully dried samples show that as the kaolin content increases, both the general level of G' and G''

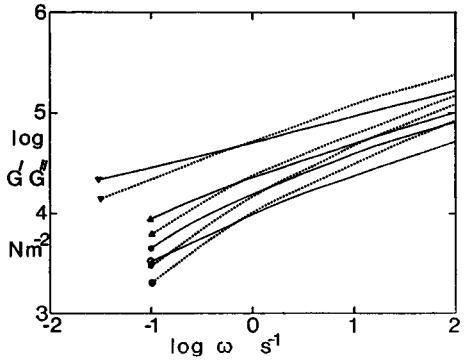

Fig. 10. Log G'' (solid lines) and G' (dashed lines) vs. log frequency for polyethylene/kaolin at 190°C: (○) $\Phi = 0$; (●) $\Phi = 0.16$; (▲) $\Phi = 0.25$; (▼) $\Phi = 0.31$.

increases and the dependence on log ω decreases. Continuous shear measurements (Fig. 11) show similar viscosity increases that vary with shear rate. In particular, there is a yield stress behavior developing for $\phi > 0.25$ at shear rates $\sim 10^{-3}$ sec^{-1}. A comparison of the viscosity enhancement factors is made with those for the Young's modulus of the system at room temperature in Figure 7. The solid modulus data are similar to those of aluminum particles in polyethylene having good adhesion.[22] The viscosity increases as a frequency or shear rate of 1 sec^{-1} are of the same magnitude. At lower frequencies and high ϕ, there is evidence of some filler "structure," but at higher frequencies/shear rates this "structure" is not operative. Micron-sized kaolin filler is an intermediate case between the much larger filler particles considered previously and the much smaller colloidal silica considered next.

Irregular-Shaped Particles

Colloidal silica in small amounts has a dramatic effect on the flow of a low-density polyethylene. Figure 12 shows that even a volume fraction of 0.005 of silica increases G'' by a factor of 1.8 at $\omega = 1$ sec^{-1}, and G' by a slightly greater amount. More significantly, at low frequencies G' no longer varies as ω^2 (as predicted by various rheological theories and found for fairly narrow MWD polymers). By $\phi = 0.02$, the low-frequency behavior of G^* has changed completely, and both components appear to be tending toward frequency-independent values as $\omega \to 0$. This is characteristic of a very weak network. The plateau value of G'' is estimated as 500 Nm^{-2} for $\phi = 0.02$. As the concentration of colloidal silica increased, this plateau level increased rapidly. This is shown by continuous shear measurements with the Weissenberg (Fig. 13) where, although the viscosity increases at low shear rates are not as great as the corresponding oscillatory results, the melt has a yield stress of ~ 1500 Nm^{-2} at $\phi = 0.05$. As an indication of the change which colloidal silica can impart to low-density polyethylene, at $\phi = 0.30$ in Alkathene WJG 11 (M.F.I. = 2), the yield stress for continuous shear flow at

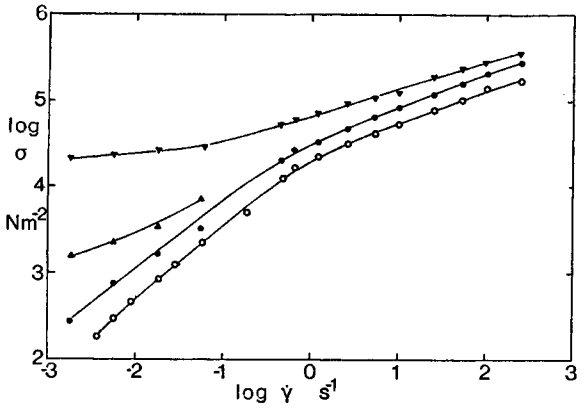

Fig. 11. Log shear stress vs. log shear rate for polyethylene/kaolin at 190°C. Symbols as in Fig. 10.

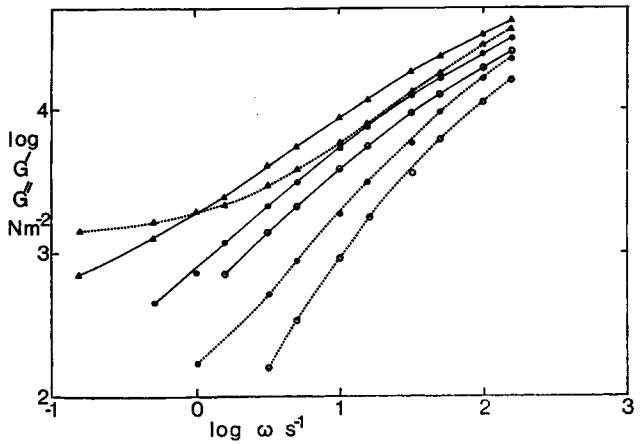

Fig. 12. Log G'' (solid lines) and G' (dashed lines) vs. log frequency for silica in polyethylene at 190°C: (○) $\Phi = 0$; (●) $\Phi = 0.005$; (▲) $\Phi = 0.02$.

190°C is $\sim 300k$ Nm^{-2} and the shear modulus G' measured with a torsion pendulum at 190°C is 6 MNm^{-2} at $\omega = 3$ sec^{-1}.

The Young's modulus enhancement factors for the system at a strain ~ 0.01 are similar to those for low-density polyethylene–kaolin (Fig. 7; the limits are one standard deviation from the mean), i.e., there is none of the dramatic viscosity increase found in the low shear rate or frequency data.

If the silica crosslinks the polyethylene chains together, the number N of crosslinks per m^3 can be calculated, using the kinetic theory of rubber elasticity, by

$$N = G/kT$$

where k is Boltzmann's constant and T is the absolute temperature. An order-of-magnitude calculation then shows that to achieve the quoted shear

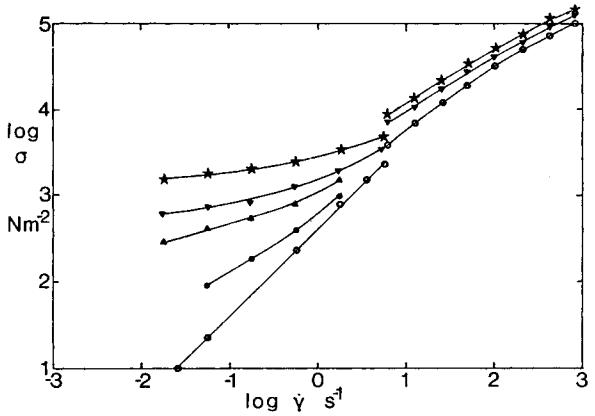

Fig. 13. Log shear stress vs. log shear rate for silica in polyethylene at 190°C: (○)Φ = 0; (●) Φ = 0.01; Φ = (▲) Φ = 0.02; (▼) Φ = 0.03; (★) Φ = 0.05. Cone-and-plate viscometer for shear rates <5 sec^{-1}, capillary viscometer results uncorrected for entrance pressure losses at higher shear rates.

modulus at low frequencies, at $\phi = 0.30$ each particle contributes 20 cross-links.

DISCUSSION

The effect of a filler on the ratio of apparent viscosities η/η_0 of the filled/unfilled polymer can change markedly with rate of shear in simple shear flow. The change is less at high frequencies in oscillatory shear flow since no overall orientation of the filler particles occurs. However, at very low frequencies the effect of weak structures formed by filler–filler or filler–polymer interaction is much greater than in simple shear flow. Therefore, the conditions for the validity of eq. (1) are:

a. The viscosities should be measured under conditions where there is no marked anisotropy of the polymer melt, i.e., for steady shear flow the shear stress should be below $\sim 10^4$ Nm^{-2}, or the flow should be approximately Newtonian. For oscillatory shear flow, there may be an advantage in making measurements in the plateau region of G'' (this means using high polymers of relatively narrow molecular weight distribution).

b. For nonspherical fillers, viscosities should be measured where the effects of weak filler structures are negligible. This rules out low shear rates/frequencies and sets an upper limit on the volume fraction of filler.

c. There should be no failure in the composite in the solid state at the strain at which measurements are made.

d. The filler size should be >1 μ, so that the surface area presented to the polymer, and hence the amount of polymer bound to the filler, should not be too great. Conversely, there should be no degradation of the polymer during incorporation of the filler.

Under the conditions when eq. (1) is valid, the filler is usually randomly oriented in space in the melt state. Variations in the filler modulus (if it is at least ten times than of the polymer) and geometry than have little effect on the modulus or viscosity ratio. Fillers of high aspect ratio have a greater effect on the viscosity than spheres, but this difference is small compared with the difference between the upper and lower shear modulus bounds of Hashin and Shtrikman. Thus, the lower bound is a reasonable approximation of the behavior of quasi-isotropic polymers containing discontinuous fillers.

The kaolinite and silica particles were of much smaller size than the other fillers studied, thus invalidating comparisons on the basis of shape alone. However, only in the case of the silica could the behavior be said to be markedly different.

It is easier in the melt state than in the solid state to obtain isotropy of the polymer and random orientation of the filler. Consequently, more confidence can be placed in melt results, and it can be predicted that in the solid state for a given concentration of randomly oriented filler, the modulus of the composite will not increase much if glass spheres are replaced by carbon fibers. There may, however, be improvements in properties such as the tensile strength of the composite. In processes such as injection molding there can be considerable orientation of both the polymer and nonspherical fillers in the final article. In such cases, the modulus ratio of the solid will be higher in some directions and lower in others than the viscosity ratio of the melt.

The theoretical problem of the viscosity of suspensions of nonspherical particles remains. In spite of the use[20] of eq. (3) for filled polymers, this approach to the problem is only valid for very dilute suspensions. For example, eq. (3) predicts that for a volume fraction of 0.2 of rods of 15:1 axial ratio, the viscosity ratio is 1400, compared to an experimental ratio of ~ 2 from Figure 4. Unless a system is Newtonian, the meaning of very low shear rate apparent viscosities is doubtful, since the data could equally well be interpreted as a strain rate-dependent yield stress.

In general, the difficulty of processing filled polymers does not increase as fast as the increase in Young's modulus with filler content. Examination of apparent viscosity data at high shear rates for the nylon fiber and kaolin systems shows that the viscosity increases are approximately given by

$$\eta_a/\eta_{a0} = 1 + \phi \qquad \phi < 0.4$$

for a shear rate of 1000 sec^{-1}. This may represent a lower limit attainable at high shear stresses since Frisch and Simha[7] quote Einstein as giving this result for the viscosity of dilute suspensions of spheres if the liquid slips over the surface. Under conditions where the apparent viscosity of a polymer decreases rapidly with increasing shear stress, this may be nearly the case.

The use of spherical fillers decreases the melt compliance (measured in oscillatory shear flow) in proportion to the increase in viscosity. Other data

in the glass transition region[23] and in the terminal flow region[24] lead to the same conclusion. It has also been concluded[20,23] that the presence of glass beads increases the glass transition temperature of the composite by about 5°C for $\phi = 0.40$. If this were true for the polystyrene system studied, then with the assumption that the viscosity is a function of $(T - T_g)$, the viscosity of the composite would have risen by an extra factor of 1.5. In fact, Figure 2 shows that the data fell below eq. (2) even without this factor. A T_g increase would shift both the G'' and G' curves in Figure 1 to lower frequencies by the same amount, so the point at which G' equals G'' would be expected to shift to lower frequencies with increasing ϕ. There is no evidence of a shift, so it appears that the glass spheres have no effect on the T_g of the polystyrene.

C. Bridle and J. Scurfield kindly supplied the polystyrene–glass sphere and polyethylene–silica samples, together with unpublished Young's modulus data on the latter. R. C. Roberts supplied the polyethylene–kaolin samples and unpublished modulus data. I am also grateful to J. W. Maddock for carrying out some of the flow measurements. The program on filled polymers was initiated by Dr. D. G. H. Ballard, and I am grateful for his support in the course of this investigation.

References

1. L. E. Nielson, *J. Compos. Mater.*, **2**, 120 (1968).
2. S. Newman and Q. A. Trementozzi, *J. Appl. Polym. Sci.*, **9**, 3071 (1965).
3. D. G. Thomas, *J. Colloid Sci.*, **20**, 267 (1965).
4. A. Einstein, *Ann. Phys.*, **17**, 549 (1905); *ibid.*, **19**, 289 (1906).
5. R. St. J. Manley and S. G. Mason, *Can. J. Chem.*, **33**, 763 (1955).
6. T. J. Farris, *Trans. Soc. Rheol.*, **12** (2), 281 (1968).
7. M. L. Frisch and R. Simha, in *Rheology*, Vol. 1, F. L. Eirich, Ed., Academic Press, New York, 1956, p. 525.
8. J. W. Robinson, *J. Phys. Coll. Chem.*, **53**, 1042 (1949).
9. M. Mooney, *J. Colloid Sci.*, **6**, 162 (1951).
10. J. G. Brodynan, *Trans. Soc. Rheol.*, **3**, 61 (1959).
11. E. H. Kerner, *Proc. Phys. Soc.*, **69B**, 808 (1956).
12. Z. Hashin and S. Shtrikman, *J. Mech. Phys. Solids*, **11**, 127 (1963).
13. A. S. Lodge, *Elastic Liquids*, Academic Press, London, 1964.
14. W. P. Cox and E. H. Merz, *J. Polym. Sci.*, **28**, 619 (1958).
15. N. J. Mills, *Rheol. Acta*, **8**, 220 (1969).
16. N. J. Mills and A. Nevin, *J. Macromol. Sci.-Phys.*, **4**, 863 (1970).
17. N. J. Mills and A. Nevin, *J. Polym. Sci. A2*, **9**, 267 (1971).
18. J. D. Ferry, *Viscoelastic Properties of Polymers*, Wiley, New York, 1961, Chap. 13.
19. A. S. Kenyon and H. J. Duffey, *Polym. Eng. Sci.*, **7**, 189 (1967).
20. D. H. Droste and A. T. Dibenedetto, *J. Appl. Polym. Sci.*, **13**, 2149 (1969).
21. J. K. Lees, *Polym. Eng. Sci.*, **8**, 195 (1968).
22. R. D. Böhme, *J. Appl. Polym. Sci.*, **12**, 1097 (1968).
23. R. F. Landel, *Trans. Soc. Rheol.*, **2**, 53 (1958).
24. M. Takano and H. Kambe, *Bull. Chem. Soc., Japan*, **37**, 89 (1964).

Received January 4, 1971
Revised June 28, 1971